Journal of Hydrology: Regional Studies 56 (2024) 102032

Contents lists available at ScienceDirect

Journal of Hydrology: Regional Studies

journal homepage: www.elsevier.com/locate/ejrh

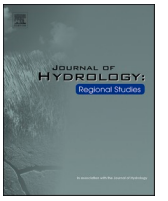

Compound effects of sea level and flow on river-induced flooding in coastal areas of southern Sweden

Fainaz Inamdeen *, Magnus Larson

Department of Water Resources Engineering, Lund University, Box 118, Lund 22100, Sweden

ARTICLE INFO

Keywords:
Flood risk
Hydraulic model
HEC-RAS
Dominance analysis
Simplified equations

ABSTRACT

Study region: Rönne River, Säve River, and Höje River, Sweden.
Study focus: River-induced flooding in coastal areas results from a multitude of drivers interacting in complex ways. The primary drivers are sea level (SL) and river flow (Q) that often exhibit coherent behavior to be considered in flood risk management. To describe and quantify the compound effects of SL and Q on flooding, a methodology was developed involving hydraulic simulations with long time series of data yielding statistical properties of output quantities such as river water level and flooded areas. Dominance analysis was conducted to quantify the relative influence of SL and Q on river water level along reaches. Also, simplified, empirically based equations were derived to predict the river water level at any location based on SL and Q.
New hydrological insights for the region: The long-term simulations revealed that the relative influence of SL and Q on the river water level changes significantly from the coast to upstream. For example, at the Rönne River, influence of SL decreases from 90 % to 20 % between 1 km and 11 km from the coast. Meanwhile, influence of Q increases from 10 % to 80 % over the same distance. The simplified equations derived to predict the water level can be used by stakeholders to forecast flood events or in risk assessment where many alternatives need to be considered.

1. Introduction

Floods are natural hazards that have been studied by scientists and engineers for centuries because of their impact on human development and related activities (Brázdil et al., 2006; Hudson and Berghäuser, 2023). In recent years, several severe flood events have occurred worldwide, causing significant loss of human lives and economic damages (Lehmkuhl et al., 2022; Sugg et al., 2023; Takayama et al., 2023; Sun et al., 2024). Most floods result from several drivers interacting (Kruczkiewicz et al., 2022; Liu et al., 2022; Yi et al., 2023) that are random in nature but possibly correlated. One such example is river-induced flooding in coastal areas, which is determined both by sea level and river runoff. In general, the variation in sea level is a function of tide, barometric pressure and wind distribution due to low-pressure atmospheric systems (typically denoted as surge or meteorological tide during storm conditions), and long-term sea level rise, which in turn exhibit the influence of a multitude of drivers. The surge component in the sea level and river runoff could display coherent behavior since they may be generated by the same meteorological event (Svensson and Jones, 2004). The importance of different drivers, their inter-relationships (Coles et al., 1999), and subsequent influence on flood characteristics are a challenge to determine and quantify, especially regarding the statistical properties of the floods.

In flood risk management (FRM), the initial step involving risk analysis requires quantification of the probability of specific flood

* Corresponding author.
E-mail address: fainaz.inamdeen@tvrl.lth.se (F. Inamdeen).

https://doi.org/10.1016/j.ejrh.2024.102032
Received 1 July 2024; Received in revised form 9 October 2024; Accepted 15 October 2024

levels and flooded areas, which constitute the basis for the following steps of risk assessment and risk reduction (Schanze, 2006; Fiori et al., 2023). If several factors are controlling the flooding, partly correlated, the statistical analysis is not straightforward, neither when it comes to the probability of occurrence for combinations of different driver values (Svensson and Jones, 2002; Moftakhari et al., 2017; Santos et al., 2021) nor for their effects on flood properties. In addition, even if the return period of such combinations can be established, and the flood properties calculated through a model, there is no guarantee that the calculated results will have the same return period as the input conditions (Olbert et al., 2023). Thus, the alternative to use long time series of input data for the drivers in a simulation model known as continuous simulations (Sopelana et al., 2018), then subject the corresponding output series to statistical analysis (Falter et al., 2016), is typically a better option. Such an approach handles the issues of correlation among drivers, their dependence, and time shifts between different drivers in a more accurate manner. However, the approach may put some limits on the spatial and temporal resolution of the modeling, since the execution time for more detailed computational models makes it difficult to simulate for long time periods needed in proper statistical treatment (c.f., Ward et al., 2011).

Currently, it is common to use one-dimensional (1D) and two-dimensional (2D) computational models to determine flood properties in water courses. Selecting between these two model types is complex, as each model offers distinct advantages depending on the specific application. For instance, 2D modeling is effective in areas with multidirectional water flow, such as flat terrain, behind levees, or in bays with tidal influences. However, 1D models can offer advantages over 2D models in some situations where flow direction is more defined and long-term or large-scale simulations are required. The decision between 1D and 2D modeling depends on factors like data availability, flow dynamics, boundary conditions, and the specific needs of the simulation (Tayefi et al., 2007; Brunner, 2024). An alternative to long-term simulations is the use of hybrid models that couple 2D computational models with advanced statistical techniques, or surrogate models that approximate complex and computationally intense simulations using machine learning algorithms (Sopelana et al., 2018; Fraehr et al., 2024). However, the accuracy of these models heavily depends on the quality of the available data and their interpolation, as well as the training and validation techniques used.

Although several studies have recently been carried out on large scales (i.e., region, country, and global) concerning the compound effects of sea level and river runoff on flooding in coastal areas (Ward et al., 2018; Camus et al., 2021; Eilander et al., 2023; Lyddon et al., 2023), they have been rather qualitative and schematic in their description, mainly emphasizing the importance of compound events and the way to proceed in the analysis at larger scales. Despite the benefits and insights provided by these studies, FRM is in general site specific and dependent on local information and high-quality data. For example, flood levels and flooded areas are

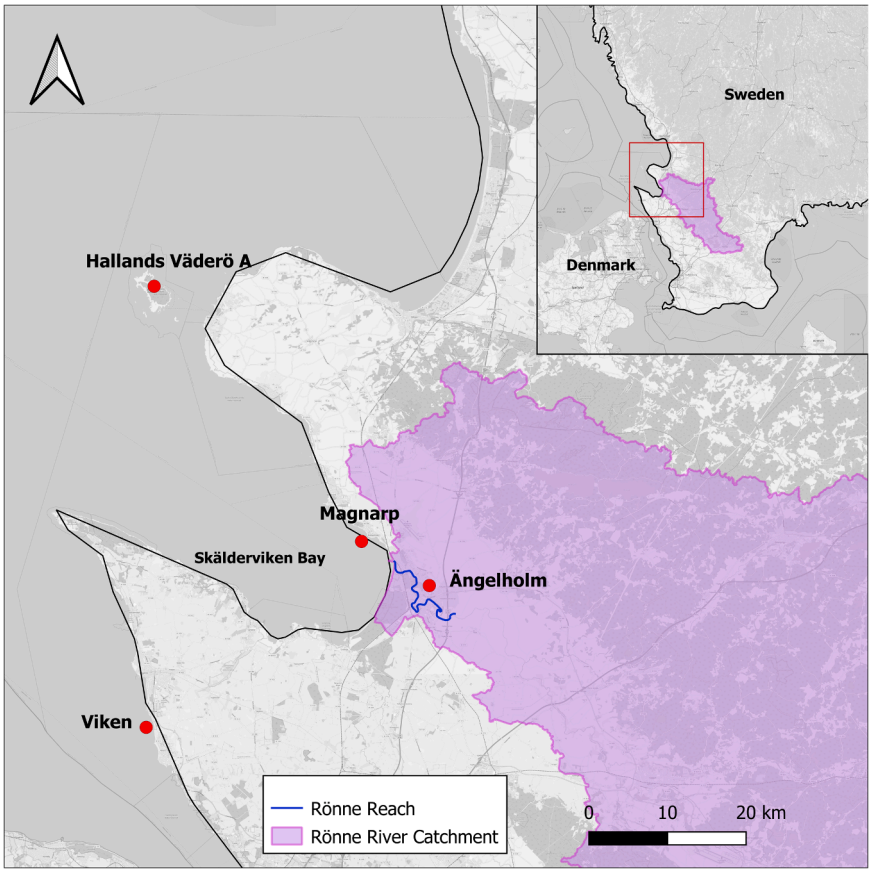

Fig. 1. Map of Rönne River catchment with sea level (Viken and Magnarp) and wind (Hallands Väderö A) measurement stations; modeled river stretch is shown. Sources: Open street map and SMHI.

functions of the bathymetry and topography for the coastal and river environment of interest, as well as adjacent land areas. Poor resolution of available elevation data severely limits the possibility of accurately quantifying the effects of a flood. In addition, model calibration and validation are needed to ensure that model results are general and applicable.

FRM studies often involve modeling since measurements of flood properties are typically limited, whereas longer series of data on the flood-generating drivers are available. Different types of modeling can also be tools to enhance and improve the communication between engineers and stakeholders (Pender and Néelz, 2007). The type of model to be employed, including how well it resolves the governing processes in time and space, will be determined by the specific focus of the FRM (e.g., Chen and Liu, 2014; Bennett et al., 2023). Also, all elements involved in the modeling procedure should be compatible, particularly the data properties in terms of availability, quality, and resolution; no model can compensate for insufficient data. Thus, the available data will typically define the limits, as well as determine the reliability and robustness, of the FRM.

The main objective of the present study was to quantify the compound influence of sea level (*SL*) and flow (*Q*) on river-induced flooding in coastal areas. A methodology was developed that involved model simulations for long time series of *SL* and *Q*, the two main drivers for flooding in the investigated cases, followed by statistical analysis of simulated flood properties such as water level and flooded area. The relative importance of *SL* and *Q* on the water level in rivers discharging to the sea was quantified for several different sites in southern Sweden.

The paper is organized as follows. First the study areas are described with focus on Rönne River, where the methodology was developed and tested, after which the main input data employed, and their properties are presented. Then the modeling procedure is outlined together with details about the hydraulic model used (HEC-RAS) and its implementation, including model calibration and validation. The model results are primarily discussed in terms of the water level along the river and flooded area, including their statistical properties. Dominance analysis was employed to display the relative importance of *SL* and *Q* for the water level variations along a river; this analysis quantifies how far up into the river the sea level should be considered. The result of applying simplified equations to directly compute the water level from *SL* and *Q* based on a set of regression equations is reviewed for the three rivers investigated. The paper ends with a set of conclusions.

2. Study areas

Rönne River has its source in Lake Ringsjön located in the central part of the most southern province of Sweden, Scania

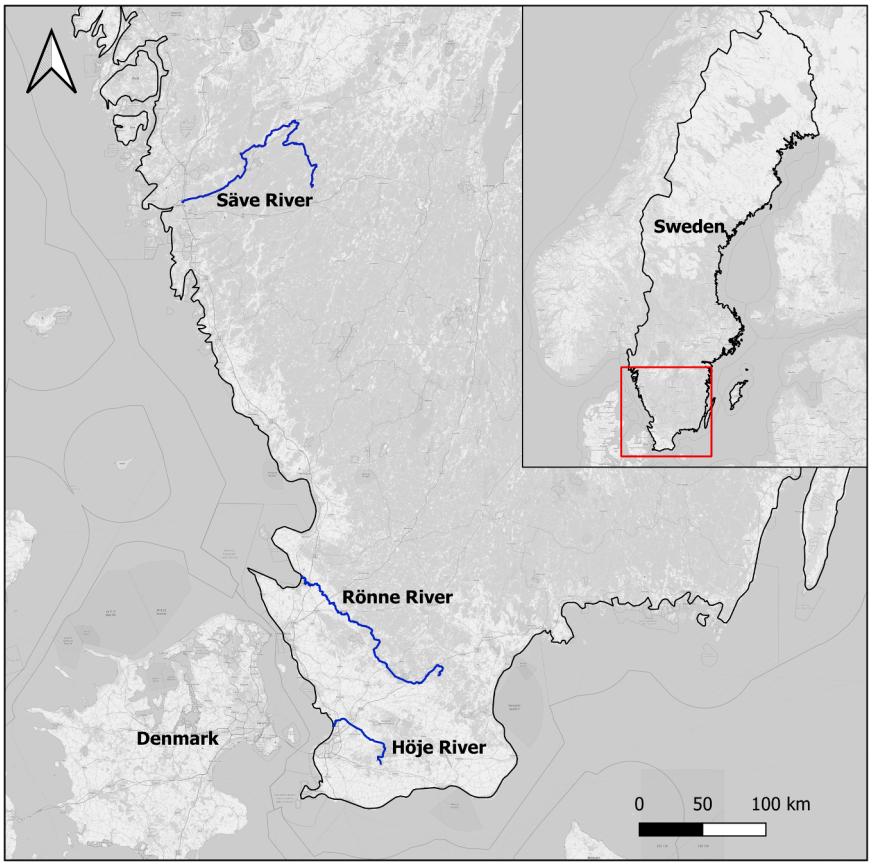

Fig. 2. Map of studied river reaches located in southern Sweden. Sources: Open street map and SMHI.

(Martin-Gousset et al., 2009). The river drains a catchment area of 1922 km^2 over a 83-km long stretch, before entering into the Skälderviken Bay near the city of Ängelholm (Fig. 1). The total length of the simulated reach in the present study is 12 km from the coastal outlet to the upstream. The downstream part of the river is characterized by many sharp meandering bends, and it typically has a distinct V-shaped cross-sectional main channel here. The longitudinal bottom profile downstream presents an average slope of 0.001. The river exhibits bed and bank erosion in several places along the studied (Inamdeen, 2020; Kalimukwa and Mohamed, 2021).

Rönne River runs through an area characterized by coastal and inland climatic conditions. The annual average temperature is 7.2 °C and the annual precipitation typically varies between 825 and 900 mm. Flows in Rönne River are in general high during winter and spring compared to summer and autumn (Persson et al., 2011a). An analysis of 39 years of simulated flow data from the Swedish Meteorological and Hydrological Institute (SMHI) shows that the study reach receives an average flow of 31.8 m^3/s during the winter and spring seasons and 15.3 m^3/s for the summer and autumn season. However, exceptional events occur; a peak flow of 209 m^3/s was encountered on the 7th of July 2007 due to severe prolonged rainfall. The second highest flow (181 m^3/s) was on the 2nd of February 2002.

Apart from Rönne River, the present study included coastal reaches of two more rivers, namely Säve River and Höje River (Fig. 2), primarily to assess the influence of sea level on river water levels and to validate the simplified approach for direct computation of the river water level from *SL* and *Q*. The Säve River is located in southwestern Sweden and flows out into the downstream part of Göta River, crossing the city of Göteborg, before discharging its water into the Kattegat Sea. The catchment area covers 1475 km^2 and the river is approximately 130 km long (Sechu, 2015). This study focuses on a 13-km section in the most downstream part of the river. The Säve catchment experiences average annual precipitation ranging from 700 mm to 1000 mm, with an average annual temperature of 6.1°C (Persson et al., 2011b).

The Höje River is situated in the western part of Scania, having a catchment area of around 316 km^2. The river is approximately 35 km long and discharges into Öresund through the city of Lomma (Betsholtz and Nordlöf, 2017). Since the Höje and Rönne River catchments are geographically close, both rivers share similar climatological and meteorological characteristics. This study has simulated a 10-km long stretch of the river from the coastal outlet. According to SMHI, over the past 40 years, several major floods were observed in all the investigated coastal river reaches. Most of these floods were close to having a 100-year return period, estimated based on fitted Gumbel distributions. Table 1 summarizes some important statistics related to flow and sea level for the studied river reaches.

Marked sea level variations along the Swedish coast are primarily influenced by storm surges caused by low-pressure atmospheric systems forming along the coast. Since 2011, Sweden has experienced over 20 storms that have significantly raised sea levels above normal values. For example, the First Advent Sunday storm on 27th November in 2011, raised the sea level at the Höje River outlet up to 1.36 m. Similarly, the storm Gorm on 29th November in 2015 increased the sea level at the Rönne River outlet up to 1.88 m (SMHI, 2024). Additional storm events and their corresponding sea levels at the Rönne River outlet are detailed in Table 2. The tidal influence on sea levels along the west coast of Sweden is markedly small (Påsse and Daniels, 2015). According to Hallin et al., (2019), the Skälderviken Bay at the Rönne River outlet experiences extreme micro tides with an average amplitude of about 5 cm, occasionally reaching 20 cm. Thus, this study did not focus on the tidal component when performing the sea level analysis.

3. Data employed and analysis

3.1. River flow and sea level

The river flow is a primary input parameter for hydraulic modeling. SMHI has simulated the flows in Rönne River by using the hydrological model S-Hype (Lindström et al., 2010; Bergstrand et al., 2014). Since there is no flow measurement station close to the study area, all flows employed originated from these simulations (SMHI 2020a). In the model simulations, daily values for the period 1981 – 2019 were used. For the other two studied river reaches (Säve River and Höje River), flow time series of daily data simulated with S-Hype for somewhat different periods was employed (2013–2019 and 2011–2019, respectively).

As shown in Fig. 1, the Magnarp station in Skälderviken Bay yielded the closest sea level measurements to the outlet of Rönne River. However, data were only available for a period from 2011/03/08–2014/05/07. Therefore, sea level measurements from the SMHI station Viken, which is located 20 km south of Skälderviken, and recorded wind speed and direction from the SMHI wind station located at Hallands Väderö were used to develop a complete sea level time series used for the hydraulic modeling from 1981 to 2019. Thus, the water level in Skälderviken Bay was determined from empirical relationships that depend on the wind conditions.

These empirical equations were developed by dividing the wind direction into eight different segments. The equations assume a

Table 1
River flow and sea level conditions in the studied reaches (flows based on simulations with the hydrological model S-Hype and water levels from measurements).

River	Average flow (m^3/s)	Maximum flow (m^3/s)	100-year return flow (m^3/s)	Closest seal level measurement station	Highest sea level ever recorded (cm)
Rönne	23.6	209	219.0	Magnarp	191.0
Säve	28.3	158.7	159.5	Göteborg-Eriksberg	165.0
Höje	3.0	36.4	32.5	Barsebäck	162.3

Note: The sea level measurement periods are different for the stations.

Table 2
The events that caused major flooding from Rönne River between 1981 and 2019.

Date	Sea level (m)	Flow (m^3/s)	Flooded area (ha)	Special remarks
29/11/2015	1.88	64.0	90.0	The storm Gorm
27/11/2011	1.91	21.0	89.1	The First Advent Sunday storm
29/01/2002	1.39	152.0	88.9	Heavy rainfall and snow melt (SMHI)
11/01/2015	1.67	99.0	88.3	The storm Egon and moderately high rainfall
06/12/2013	1.84	34.0	87.7	The storm Sven
07/07/2007	0.43	209.0	87.0	Heavy rainfall (SMHI)

quadratic dependence on the wind speed, since wind setup is related to the surface shear stress that is a function of the square of the wind speed. The main coefficients in these equations reflect the geometry of the bay, including the fetch length for the actual wind direction. The difference between recorded sea levels at the Magnarp and Viken Stations for the common measurement period was analyzed regarding wind speed and direction through regression analysis, and different relationships were established for each segment with specific coefficient values based on the equation $M.SL = V.SL + aW^2$, where $M.SL$ = Magnarp sea level, $V.SL$ = Viken sea level, W = wind speed, and a = coefficient that depends on the wind direction.

The tidal effects are quite small but noticeable. The water level data for Viken Station were acquired through the SMHI open data portal (SMHI 2020b), encompassing hourly values. Similar data were available for the other studied river reaches, but no local corrections were needed in these cases, since the measurement stations were closer to the river outlets and more representative. Although the sea level measurements were available on an hourly basis, the daily maximum value was employed in simulations to yield the expected highest river level for a particular day.

Fig. 3 displays a scatter plot of the sea level inside Skälderviken Bay versus the flow in Rönne River for the studied 39-year time series (daily values). The plot indicates some interrelationship between SL and Q, but the correlation is low and quantifying this dependency is difficult, especially for the more extreme events that cause major flooding. The six most prominent events in terms of generating the largest flooded areas are marked red in the figure, to be discussed more in a later section. The locations of these events in the plot seem to fall beyond a certain envelope defined by a combination of SL and Q that decreases monotonically, with lower sea levels being compensated by higher flow to produce a specific event with a certain return period. The simplified empirical equations developed later in the paper may be used to approximately define such envelope curves (example of such curves are shown in Fig. 3 for

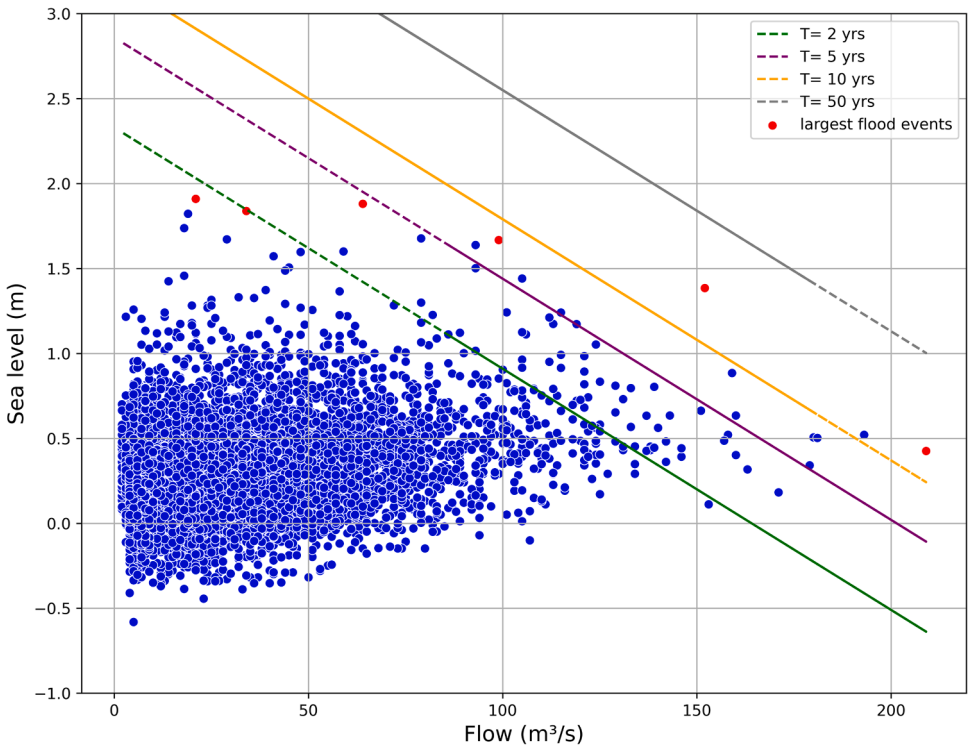

Fig. 3. Scatter plot of measured sea level versus simulated river flow in the downstream part of Rönne River, where the events generating the six largest flooded areas are marked together with envelope curves defining combinations of sea level and river flow that cause a certain water surface elevation at a location 6000 m upstream the river mouth (curves derived from simplified empirical equations); sea level measurements are based on the RH2000 elevation system.

river water levels at a specific location).

3.2. Bathymetry and topography

Hydraulic models require detailed, accurate bathymetric and topographic data to produce reliable estimates of hydraulic characteristics in connection with the modeling of floods (cf., Stoleriu et al., 2020). In this study, a high-resolution digital elevation model was compiled by combining river bathymetric data and topographic data for Rönne River. Multibeam echo sounding (MBES) technology was used for the underwater (bathymetric) survey and Light Detection and Ranging (LiDAR) for the survey above water, describing the banks of the river. The survey was conducted along a 12-km river stretch starting at the outlet at Skälderviken Bay and ending at a bridge crossing the road E6. The vertical measurement uncertainty is about ± 4.5 cm for a depth of 10 m from the measuring point (MTE, 2020). The data sets aligned with the SWEREF 99 1330 coordinate system and the RH 2000 reference elevation plane with a 0.5 m spatial resolution. The topographic data for the extended flood plains were obtained from the Swedish Land Survey national model with 2 m spatial resolution (from LiDAR surveys) and combined with the river survey data. The topographic data show absolute positional accuracy of at least 0.3 m in the plane and 0.1 m in elevation (Lantmäteriet, 2022).

The bathymetric and topographic data for the other river reaches were obtained from previous modeling studies (MSB, 2015; Sechu, 2015), typically encompassing less detailed measurements of the riverbed and banks than for Rönne River.

4. Modeling river flow and subsequent analysis

4.1. Modeling approach and implementation using HEC-RAS

The HEC-RAS model (Brunner, 2016; Čepienė et al., 2022; Sarchani and Tsanis, 2024) was used to simulate river hydraulics including a varying sea level, employing a one-dimensional (1-D), quasi-steady approach and establishing 270 river cross-sections to represent the bathymetry/topography of the 12-km Rönne River reach. Quasi-steady refers to input conditions changing with time, but where simulations within each time step assume steady conditions. Such an assumption allows for rapid solution of the governing equations where long time series of input data can be handled at rather modest execution times, which was critical in the present study. Thus, some limits exist to spatial and temporal scales being properly resolved in the modeling and their coupling. The length of the river reaches modeled were such that it may be assumed that steady-state conditions develop during the time step of interest (one day), making the present approach satisfactory. However, for much longer river stretches, or rapidly varying flow, time-varying formulations will be necessary.

The variation in the input flow conditions is the result of runoff from a large catchment, implying a gradual variation in the flow on a daily time scale. However, the sea level is changing more rapidly, typically on an hourly time scale, but these changes are also rather gradual, and the studied river stretch sufficiently short to respond in a manner compatible with a quasi-steady approach (it takes about half an hour for a small disturbance to propagate from the river outlet to the upstream end of the reach at Rönne River).

Thus, the daily river flow obtained from SMHI was used as upstream input, and the derived daily maximum sea level at Magnarp as the downstream boundary condition. The water level along the river and the flooded area were the key outputs from the model simulations subjected to further analysis, although other hydraulic parameters such as velocity and shear stress were also available. For the Rönne River, numerical simulations were conducted over a 39-year period from 1981 to 2019, resulting in over 14,000 simulations

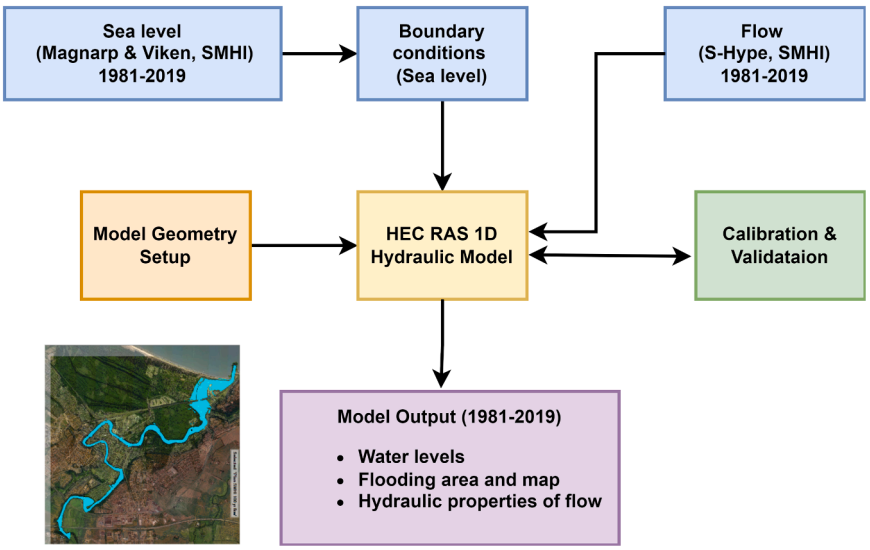

Fig. 4. Workflow chart for the HEC-RAS 1D model simulations.

on a daily time scale. Fig. 4 schematically illustrates the work flow for the HEC-RAS 1D model simulations. In the cases of Höje River and Säve River, hydraulic simulations were performed using model setups developed in previous studies. A 10-km HEC-RAS 1D model was created for Höje River by converting a MIKE 11 model developed by MSB (2015), and the simulations were conducted over the period 2011–2019. For Säve River, a 13-km HEC-RAS 1D model from Sechu (2015) was employed to perform hydraulic simulations for the period 2013–2019. The HEC-RAS 1D models for both Höje and Säve Rivers were not specifically calibrated and validated in this study, since this had already been done in the previous applications.

4.2. Calibration and validation

In the calibration process of hydraulic modeling, the value of the roughness coefficient is typically adjusted by fitting simulated water surface elevations (WSE) to observed elevations at different locations (Brunner, 2016; Pinos and Timbe, 2019; Bessar et al., 2020). In this study, for model calibration and validation, the daily maximum water level measured at Pyttebron (a bridge), located about 4.5 km upstream of the coastal outlet was compared to the corresponding water level simulated by the HEC-RAS model for the period from 2011/03/08–2014/05/07. This period was selected since sea level measurements were available at the Magnarp Station (set as the downstream boundary condition), avoiding additional uncertainty in the model input resulting from using the empirical equations to account for the local wind setup when the Viken Station is used. The first year in the studied period was used for calibration, whereas the remaining period (about two years) was employed for validation.

For simplicity, the main channel and the flood plain roughness conditions were assumed to be uniform but different, resulting in optimal calibrated values for the Manning coefficient of 0.028 and 0.040, respectively. Figs. 5 and 6 illustrate the performance of the model for the entire period by comparing simulated and measured water levels. Fig. 6 illustrates the results for the calibration and validation periods, where the coefficient of determination (R^2) for the calibration period is 0.95 and for the validation period 0.92. The similarity of these two values indicates a satisfactory model validation. In addition, the root-mean-square error (RMSE) and mean bias error (MBE) were computed for both the calibration and validation phases to further assess the hydraulic model performance. The RMSE and MBE values were 0.07 and −0.030 for the calibration, and 0.07 and −0.035 for the validation, respectively. These results suggest that the errors in both calibration and validation are relatively low, with a slight negative bias indicating that the simulations tend to slightly overpredict the measurements on average. However, this bias is minimal and does not significantly impact the overall accuracy of the model.

4.3. Dominance and extreme value analysis

Dominance Analysis (DA) was used to find the relative, overall influence of *SL* and *Q* on the river water level along the studied reaches. The original theory was introduced by Azen and Budescu (2003), whereas the program employed here for the DA was developed by Shekhar et al., (2018). DA computes the percentage relative importance of the predictors based on pseudo R-squared (R^2) contribution of the individual, average partial, and interactional dominance of the predictors through multiple regression analysis (Shekhar et al., 2018).

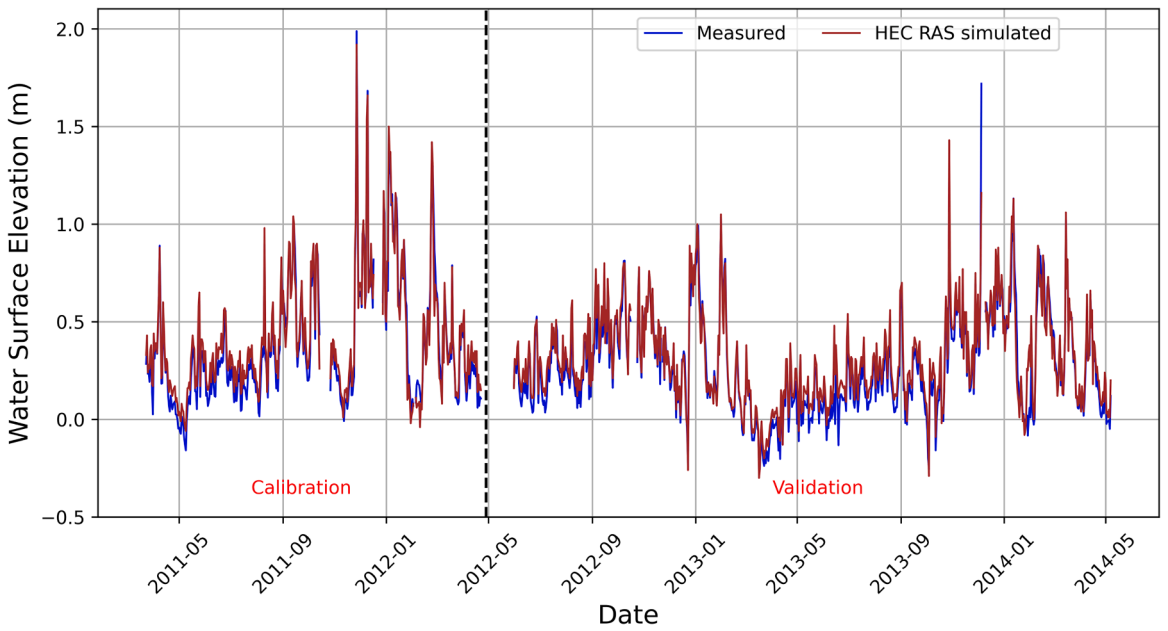

Fig. 5. Comparison of observed and simulated water levels (daily maximum) at Pyttebron in Rönne River.

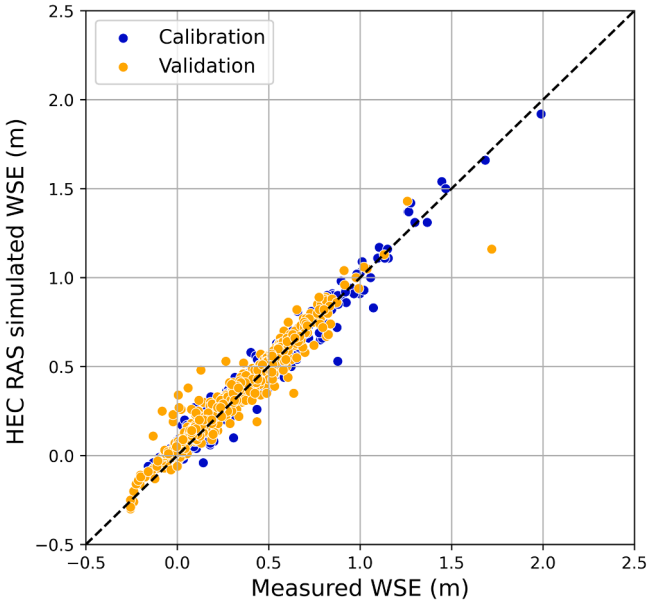

Fig. 6. Scatter plot of observed versus simulated water level at Pyttebron in Rönne River for the calibration and validation periods.

The statistical program R (R Core Team, 2013) was used for frequency analysis of river flow, sea level, and different output quantities from the model simulations (e.g., river water levels, flooded area). A special package called extRemes with graphical user interface in2extRemes (Gilleland, 2020) was employed for the extreme value analysis (EVA) by considering a suitable distribution of

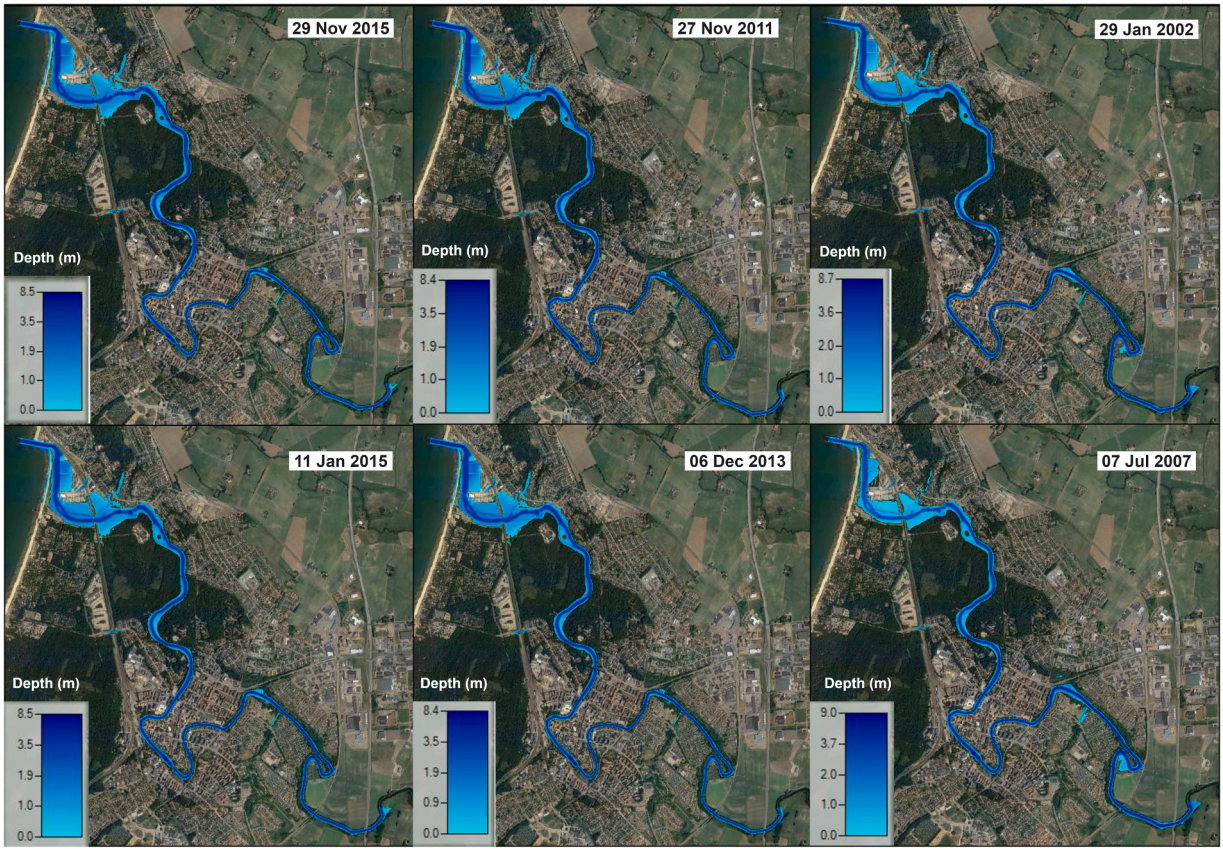

Fig. 7. Simulated flooded area for some extreme events recorded during the period 1981–2019 as described in Table 2.

block maxima (Coles, 2001).

5. Results

5.1. Flooded area

The inundation maps obtained from the HEC-RAS simulations show the spatial extent of flooding along the river reach for the simulation period of 39 years. The *SL* data used in this study represent daily maximum values, whereas the *Q* data are provided on a daily scale. The simulation results clearly illustrate the dependence of the flooded area on both *SL* and *Q*, and how the inundated area changes according to their compound influence. A maximum simulated flooded area of 90 ha was obtained on 29 Nov 2015 when the storm Gorm hit southwest Sweden. At that time the maximum recorded gust wind speed at Hallands Väderö was about 40 m/s, an event with a predicted return period of just over 25 years (SMHI, 2015). In comparison, the flooded area (i.e., covered by water) for average flow and mean sea level is about 43 ha. Table 2 summarizes basic information about the six events that caused the largest floods along the studied reach. Fig. 7 illustrates the inundation maps for these events. The major flood-prone areas are in the downstream part of the river stretch, where low-lying areas are present. The complex relationship between *SL* and *Q* causing the flooding is clearly indicated by the simulations.

As an example of the interaction between *SL* and *Q*, in July 2007 the Rönne River basin experienced unusually heavy rainfall with the highest flow being 209 m^3/s in the downstream reach. The monthly rainfall was over 200 mm, which is 250 % higher than the average precipitation in July. However, due to rather normal sea level conditions, the water levels were not the most extreme in the downstream part of the river during this period.

Fig. 8 shows a comparison between the water surface elevations (WSE) for the six major events summarized in Table 2. Although the inundated area only showed slight differences among these events, the plotted WSE clearly displays the effect of sea level and flow on the water levels in the river, as well as the flooding extent spatially. High sea levels cause flooding in the downstream part of the river, whereas high flows cause similar floods in the upstream part. Note that the six largest flood events typically do not correspond to the six events with the largest WSE at a specific location.

EVA was performed regarding the annual maximum flooded area extracted from the simulated time series with HEC-RAS. A generalized extreme value distribution was fitted to the data and the optimum parameters estimated using a maximum likelihood approach. The optimum shape parameter indicated that a Gumbel distribution fits well and was the preferred distribution to employ, which was also confirmed by comparing the Akaike and Bayesian information criteria for different distributions (Laio et al., 2009). By using the simulated data from a long time series, the compound effects on the flooding were properly represented and the EVA became straightforward yielding appropriate return periods for the flooded area.

5.2. Influence of sea level and flow on river water level

The influence of *SL* and *Q* on river water levels in the studied coastal reaches was determined through DA based on the entire simulation period and at different locations. For Rönne River, the results show that the sea level in Skälderviken Bay affects water levels throughout the 12-km reach from the coast, although the influence is largest downstream. The influence of *SL* and *Q* has almost equal effect around 5 km from the coast (see Fig. 9).

Similarly, DA was carried out for the studied coastal reaches of Säve River and Höje River. For Höje River, a 10-km HEC-RAS 1D

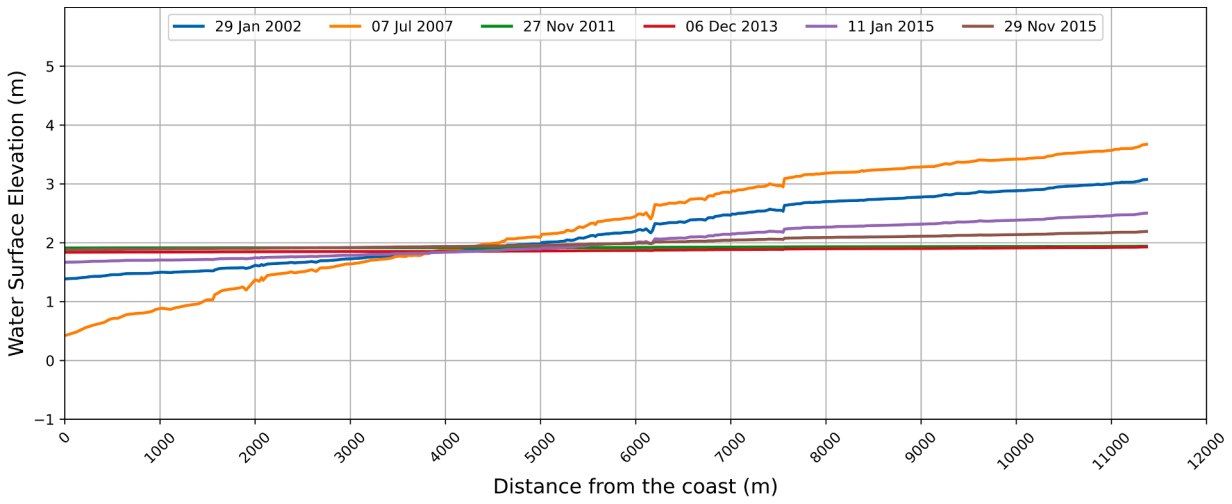

Fig. 8. Simulated water surface elevation along Rönne River reach for six major flooding events recorded during the period 1981–2019 as described in Table 2.

model was developed by converting a MIKE 11 model developed by MSB (2015). For Säve River, a 13-km HEC-RAS 1D model was employed from (Sechu, 2015), who in a previous modeling study focused on sediment transport and erosion in the river. In the case of both Höje and Säve Rivers, the influence of sea level is dominant downstream, and from about 6 km the flow mainly influences the water level (Fig. 10).

5.3. Simplified modeling procedure

To develop a simplified method to predict river water levels, multiple linear regression analysis was performed by using WSE acquired from model simulations versus corresponding input of *SL* and *Q*. For that, 45 different model simulations were used by combining various *SL* and *Q*. The flows were selected in the range between maximum and minimum input flows. Similarly, sea levels were chosen between high and low observed values (above MSL). The approach taken is similar to developing a stage-discharge curve (Herschy, 1998) often used in engineering hydrology, but where the WSE in the river is obtained from the flow (and not vice versa) and also includes the sea level (cf., Jones et al., 2019; Lee et al., 2021). In addition, the data for the curve was obtained from a validated numerical model and not actual measurements (Rantz, 1982). The empirical equations derived were of simple, algebraic type to allow for easy application, as opposed to presenting relationships in graphical form, employing advanced statistical methods in the data analysis (e.g., Le Coz et al., 2014). Since the equations are derived from the quasi-steady modeling, gradual variations are assumed and dynamic effects are not included (Dottori et al., 2009).

Based on simple theory and previous studies, it is noted that when the flow is completely dominant, the WSE follows the flow to a certain power. However, if both *SL* and *Q* influence the water level, it was observed in the present study that a linear equation yields satisfactory results. In the case of Rönne River, the developed set of simplified equations were linear over the entire studied reach ($y = a + bSL + cQ$, where y is WSE in the river, SL sea level, Q flow, and a, b, c are empirical coefficients valid for a particular location; specific values are not given here). However, for the Höje River and Säve River cases, the simplified equations were only linear in the downstream part of the reach; when influence of sea level was negligible further upstream, power equations based on the flow yielded better agreement ($y = cQ^m$, where m is an empirically determined power).

Fig. 11 illustrates predictions of the WSE based on HEC-RAS simulations and using simplified equations for different locations along the Rönne, Höje, and Säve River reaches, including the values on the coefficient of determination. The accuracy of the simplified equations for each river was evaluated using the coefficient of determination (R^2), root-mean-square error (RMSE), and Mean Bias Error (MBE). For Rönne River, the validity of the empirical equations was investigated by comparing 39 years (1981–2019) of simulated WSE with estimated WSE from the simplified linear equations when the sea level was above 0.0 m (focus was on higher river water levels). It is acknowledged that for cases with combinations of very high sea level and very low flow, and very low sea level and very high flow, the simplified method provides less good agreement.

An extreme value analysis was performed using the Gumbel distribution on 39 years (1981–2019) of simulated WSE and the WSE estimated from the simplified equations for the Rönne River, see Table 3. The objective of this analysis was to quantify the error in cases where the variation in WSE is low. The MBE for location KP 4000 is 0.08 m, for location KP 7500 0.04 m, and for location KP 11000 -0.001 m. Overall, the MBE suggests that the simplified equations yield relatively low errors, indicating their effectiveness in

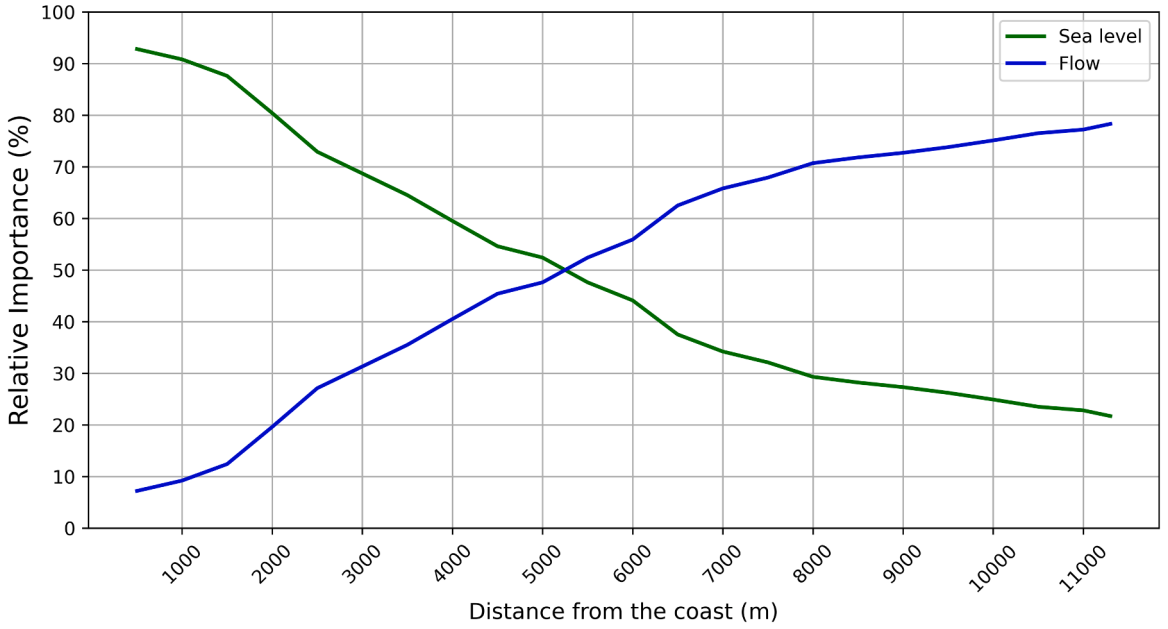

Fig. 9. The relative importance of sea level and flow on water levels along the studied Rönne River reach determined through dominance analysis.

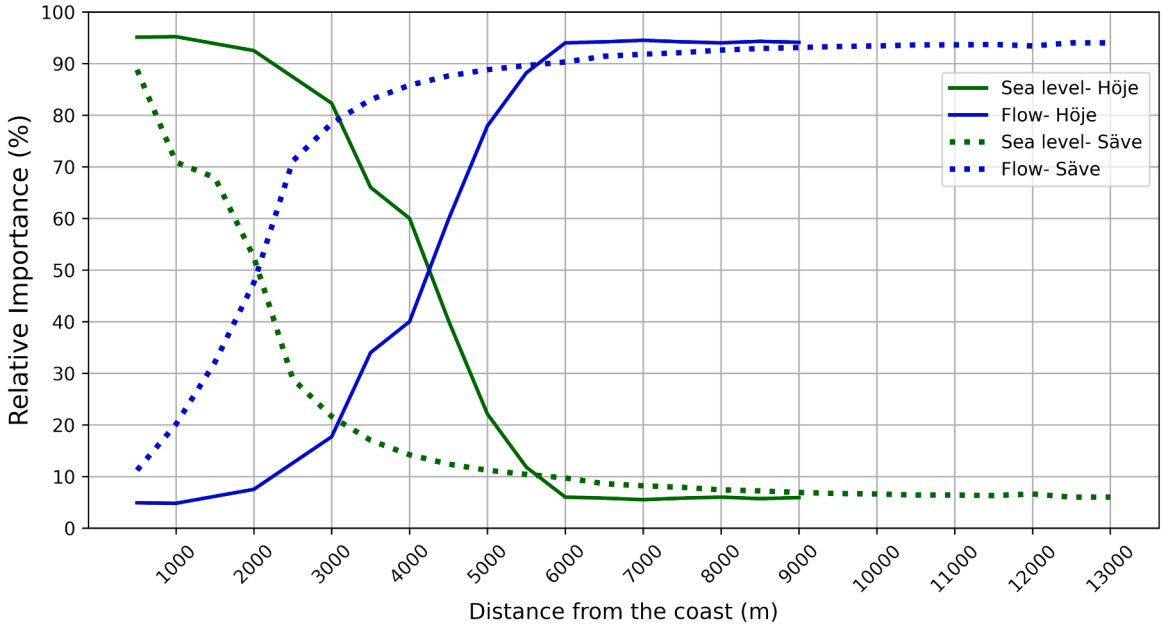

Fig. 10. The relative importance of sea level and flow on water levels along the studied Höje and Säve River reaches determined through dominance analysis.

estimating WSE with low variation.

For Höje River, the validity of the simplified equations was investigated with nine years of simulated WSE from HEC-RAS (2011–2019) when sea level was above 0.0 m and flow was greater than 2 m^3/s. For Säve River, the validity was checked with seven years (2013–2019) for sea levels above 0.0 m. In general, Höje River flows are lower than for the other two studied rivers; when the flow is very low, the simplified equations yield higher uncertainties in the water level predictions. In Säve River for cases involving combinations of very high sea level and very low flow, and very low sea level and very high flow, the uncertainty is larger. For both Höje and Säve reaches, power equations were used for distances of more than 6 km upstream the river outlet.

The simplified equations represent the combined effects of *SL* and *Q* on the WSE, thus making it possible to use these equations to derive a return period for a specific WSE event in terms of the two drivers. As example, Fig. 3 includes curves for different return periods regarding the WSE 6000 m upstream the mouth of the Rönne River using the simplified equation. From these curves it is possible to identify combinations of *SL* and *Q* that yield a specific WSE at a certain location considering compound effects. However, it should be noted that although the fit of the simplified equations to the HEC-RAS simulations are typically satisfactory, extreme events might not be as well represented, but rather an overall agreement with the simulation results is achieved. Thus, the simplified equations may fail to accurately describe events with longer return periods, if these equations do not agree well with the simulations for the more extreme events.

6. Discussion

The methodology developed in this study can be adapted and implemented in other river sections near coastal areas with similar characteristics. The general input parameters needed to develop a hydraulic model and subsequent simplified equations, along with the resulting output parameters, are summarized in Table 4.

Sea level rise may be important to consider, especially in the context of ongoing climate change. The global sea level has risen by an average of 15–25 cm between 1901 and 2018, with variations across different regions (Fox-Kemper et al., 2021). In Sweden, the average sea level rise since 1900 is approximately 15 cm, moderated by the effects of land mass uplift (SMHI, 2022). However, climate change projections indicate that global sea levels could rise by 63–101 cm at the end of the 21st century under the SSP5–8.5 scenario (Fox-Kemper et al., 2021). The SMHI sea level measurements show that the mean sea level near the Rönne River outlet increased by 8.1 cm between 1981 and 2019. The present study utilized measured sea level data that already captured this rising trend, incorporating it as a boundary condition in the hydraulic simulations. The projected sea level rise for a specific region can easily be incorporated into the developed site-specific simplified equations when determining water levels along the river. The Swedish coast experiences low amplitude astronomical tides, so these were not a major focus in the present analysis. However, if this methodology is applied to a coastal region where astronomical tides are significant, they should be carefully considered and incorporated into the modeling.

In this study, a 1D model was used due to the need for long-term simulations when evaluating the flood properties. Utilizing a 2D model would have required more processing time, as well as more detailed input data not available, for this application. However, the

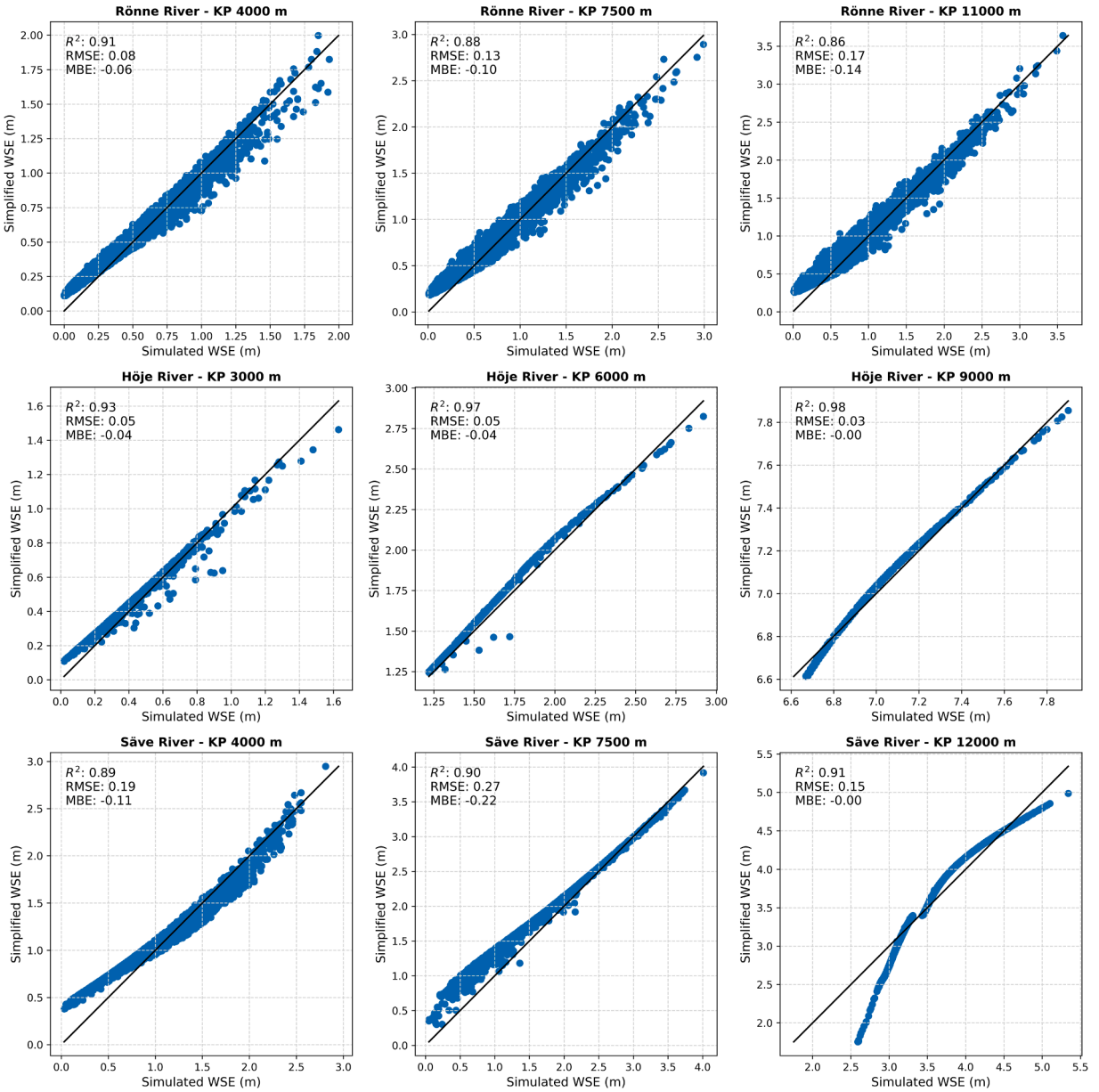

Fig. 11. Scatter plots of water surface elevation from HEC-RAS simulations and predictions with simplified equations at different locations along the Rönne, Höje and Säve River reaches (KP refers to the distance from the river mouth going upstream).

Table 3
Extreme value statistics of simulated and simplified water surface elevation for selected locations in Rönne River.

Location	KP 4000 m		KP 7500 m		KP 11000 m	
Return period	WSE simulated (m)	WSE simplified (m)	WSE simulated (m)	WSE simplified (m)	WSE simulated (m)	WSE simplified (m)
2	1.41	1.34	1.82	1.76	2.13	2.08
5	1.67	1.60	2.23	2.18	2.62	2.59
10	1.85	1.78	2.50	2.45	2.95	2.94
25	2.08	1.99	2.84	2.80	3.37	3.37
50	2.24	2.15	3.09	3.06	3.67	3.69
100	2.41	2.32	3.34	3.32	3.98	4.01
200	2.57	2.48	3.60	3.57	4.28	4.33

Table 4
The input and output parameters relevant for hydraulic simulations and simplified equations in the present study.

Model application	HEC RAS Hydraulic model	Simplified equations
Input parameters	River flow	River flow
	Sea level (tide, surge)	
	Bathymetry	Sea level
	Topography	
	Roughness coefficient	
Output parameters	Water surface elevation	Water surface elevation
	Flooded area	
	Flow velocity	Flooded area
	Shear stress	

study acknowledges that in areas with flat terrain and rapid response, which are different from the case study locations included here, employing a 2D model or a combination of 1D and 2D models would enhance accuracy in the simulations and for the development of the simplified equations.

7. Conclusions

The main objectives of the present study were to develop and validate a methodology to quantify the compound effects of *SL* and *Q* on river-induced flooding in coastal areas, where statistical measures of flood properties to be used in risk analysis are properly estimated. The approach taken encompassed simulations with the hydraulic model HEC-RAS for a long time series of input data on *SL* and *Q*, yielding a corresponding output that was subjected to statistical analysis. The alternative to describe the joint probability of occurrence for the drivers of flooding, including their inter-relationships and possible time shifts, followed by the use of a simulation model, presents theoretical challenges. In addition, return periods derived for combinations of drivers do not typically produce model outputs having the same statistical properties.

The methodology was implemented for three rivers in southern Sweden, where detailed data on sea level, flow, and river bathymetry and topography were available, with special focus on Rönne River. The output from the long-term simulations displayed the complex relationship between the variation in the main drivers (e.g., *SL* and *Q*) and the flood properties. Similar areas of flooding were observed for large sea levels and ordinary flows as for ordinary sea levels and large flows, although the specific location of the flooding varied. Overall, the investigation indicated the difficulties in performing statistical analysis of the drivers for flooding that will define events with specific return periods relevant for the flood properties.

Dominance analysis was also carried out for the three studied river reaches to quantify the average influence of *SL* and Q on the river water level moving from the outlet and upstream. This type of analysis will reveal how far upstream in coastal river reaches that the sea level needs to be considered in hydraulic simulations. Finally, simplified equations were derived from HEC-RAS simulations to predict the river water level at any location from *SL* and *Q*. Such equations may be used by stakeholders to forecast flood events or in risk assessment where many alternatives need to be considered.

In summary, the methodology employed worked well and was efficient for the study sites included, producing the results needed for the specific cases discussed. The methodology has a potential for application to sites with similar characteristics as the ones involved in the present study. It is recognized that the present study involved several limitations that will require additional efforts in terms of data, modeling, and subsequent analysis if they are to be overcome. For example, here a quasi-steady approach was taken, assuming that the studied reach was sufficiently short, and the input flow slowly varying, to allow for equilibrium to occur during a specific flow time step.

CRediT authorship contribution statement

Fainaz Inamdeen: Writing – original draft, Methodology, Investigation. **Magnus Larson:** Writing – original draft, Supervision.

Declaration of Competing Interest

The authors declare that they have no known competing financial interests or personal relationships that could have appeared to influence the work reported in this paper.

Acknowledgements

The authors appreciate the financial support from the Swedish Civil Contingencies Agency (MSB) and the Swedish Research Council for Sustainable Development (FORMAS) as part of the project ”EXTREME-INDEX” (grant number MSB 2019–06053) as well as from the Swedish Transport Administration (Trafikverket) through the project ”Impact of extreme river flows on bridges with special focus on local scour” (grant number BBT 2021–013). In addition, FI would like to acknowledge support from Lundbergsstiftelserna and Åke och Greta Lissheds Stiftelse, and ML from STINT (grant number JA2017–7011) for funding a research visit to the University of Tokyo. The Municipality of Ängelholm kindly provided bathymetric data för Rönne River, whereas Dr. Gasper Sechu transferred his

HEC-RAS input data for Säve River. The constructive and valuable comments provided by the Editor and the anonymous reviewers are greatly appreciated.

Data Availability

Data will be made available on request.

References

Azen, R., Budescu, D.V., 2003. The dominance analysis approach for comparing predictors in multiple regression. Psychol. Methods 8 (2), 129.

Bennett, W.G., Karunarathna, H., Xuan, Y., Kusuma, M.S., Farid, M., Kuntoro, A.A., Rahayu, H.P., Kombaitan, B., Septiadi, D., Kesuma, T.N., 2023. Modelling compound flooding: a case study from Jakarta, Indonesia. Nat. Hazards 118 (1), 277–305.

Bergstrand, M., Asp, S.-S., Lindström, G., 2014. Nationwide hydrological statistics for Sweden with high resolution using the hydrological model S-HYPE. Hydrol. Res. 45 (3), 349–356.

Bessar, M.A., Matte, P., Anctil, F., 2020. Uncertainty analysis of a 1d river hydraulic model with adaptive calibration. Water 12 (2), 561.

Betsholtz, A. and B. Nordlöf 2017. Potentials and limitations of 1D, 2D and coupled 1D-2D flood modelling in HEC-RAS. TVVR17/5003.

Brázdil, R., Kundzewicz, Z.W., Benito, G., 2006. Historical hydrology for studying flood risk in Europe. Hydrol. Sci. J. 51 (5), 739–764.

Brunner, G.W., 2016. HEC-RAS River Analysis System: Hydraulic Reference Manual Version 5.0. US Army Corps of Engineers-Hydrologic Engineering Center (HEC), Davis, CA, USA.

Brunner, G.W., 2024. HEC-RAS River Analysis System: HEC-RAS 2D User's Manual Version 6.5. US Army Corps of Engineers-Hydrologic Engineering Center (HEC), Davis, CA, USA.

Camus, P., Haigh, I.D., Nasr, A.A., Wahl, T., Darby, S.E., Nicholls, R.J., 2021. Regional analysis of multivariate compound coastal flooding potential around Europe and environs: sensitivity analysis and spatial patterns. Nat. Hazards Earth Syst. Sci. 21 (7).

Čepienė, E., Dailidytė, L., Stonevičius, E., Dailidienė, I., 2022. Sea level rise impact on compound coastal river flood risk in Klaipėda city (Baltic Coast, Lithuania). Water 14 (3), 414.

Chen, W.-B., Liu, W.-C., 2014. Modeling flood inundation induced by river flow and storm surges over a river basin. Water 6 (10), 3182–3199.

Coles, S., 2001. An Introduction to Statistical Modeling of Extreme Values. Springer-Verlag, London, United Kingdom.

Coles, S., Heffernan, J., Tawn, J., 1999. Dependence measures for extreme value analyses. Extremes 2, 339–365.

Dottori, F., Martina, M., Todini, E., 2009. A dynamic rating curve approach to indirect discharge measurement. Hydrol. Earth Syst. Sci. 13 (6), 847–863.

Eilander, D., Couasnon, A., Leijnse, T., Ikeuchi, H., Yamazaki, D., Muis, S., Dullaart, J., Haag, A., Winsemius, H.C., Ward, P.J., 2023. A globally applicable framework for compound flood hazard modeling. Nat. Hazards earth Syst. Sci. 23 (2), 823–846.

Falter, D., Dung, N., Vorogushyn, S., Schröter, K., Hundecha, Y., Kreibich, H., Apel, H., Theisselmann, F., Merz, B., 2016. Continuous, large-scale simulation model for flood risk assessments: Proof-of-concept. J. Flood Risk Manag. 9 (1), 3–21.

Fiori, A., Mancini, C., Annis, A., Lollai, S., Volpi, E., Nardi, F., Grimaldi, S., 2023. The role of residual risk on flood damage assessment: a continuous hydrologic-hydraulic modelling approach for the historical city of Rome, Italy. J. Hydrol.: Reg. Stud. 49, 101506.

Fox-Kemper, B., H. Hewitt, C. Xiao, G. Aðalgeirsdóttir, S. Drijfhout, T. Edwards, N. Golledge, M. Hemer, R. Kopp and G. Krinner 2021. Ocean, cryosphere and sea level change. Climate change 2021: the physical science basis. Contribution of Working Group I to the Sixth Assessment Report of the Intergovernmental Panel on Climate Change. P. Zhai, editor;, A. Pirani, editor.

Fraehr, N., Wang, Q.J., Wu, W., Nathan, R., 2024. Assessment of surrogate models for flood inundation: the physics-guided LSG model vs. state-of-the-art machine learning models. Water Res. 252, 121202.

Gilleland, E. 2020. Package 'extRemes': Extreme Value Analysis. R package version 2.1. Accessed December,1 2020. ⟨https://CRAN.R-project.org/package=extRemes⟩.

Hallin, C., Almström, B., Larson, M., Hanson, H., 2019. Longshore transport variability of beach face grain size: implications for dune evolution. J. Coast. Res. 35 (4), 751–764.

Herschy, R.W., 1998. Stage-discharge relation. Encyclopedia of Hydrology and Lakes. *Encyclopedia of Earth Science*. Springer, Dordrecht, pp. 631–634.

Hudson, P., Berghäuser, L., 2023. Investigating moral hazard and property-level flood resilience measures through panel data from Germany. Int. J. Disaster Risk Reduct. 84, 103480.

Inamdeen, F., 2020. Evaluation of Local Scour along Rönne Å at Ängelholm. Master Thesis, TVVR 20/5019, Division of Water Resources Engineering, Department of Building and Environmental Technology. Lund University, Lund,Sweden.

Jones, A.E., Hardison, A.K., Hodges, B.R., McClelland, J.W., Moffett, K.B., 2019. An expanded rating curve model to estimate river discharge during tidal influences across the progressive-mixed-standing wave systems. Plos One 14 (12), e0225758.

Kalimukwa, A.M., Mohamed, A.J., 2021. Evaluation of bank erosion and stability analysis along Rönne å at Ängelholm, Sweden. Master Thesis TVVR 21/5011, Division of Water Resources Engineering, Department of Building and Environmental Technology. Lund University, Lund, Sweden.

Kruczkiewicz, A., Cian, F., Monasterolo, I., Di Baldassarre, G., Caldas, A., Royz, M., Glasscoe, M., Ranger, N., van Aalst, M., 2022. Multiform flood risk in a rapidly changing world: what we do not do, what we should and why it matters. Environ. Res. Lett. 17 (8), 081001.

Laio, F., Di Baldassarre, G., Montanari, A., 2009. Model selection techniques for the frequency analysis of hydrological extremes. Water Resour. Res. 45, W07416.

Lantmäteriet, 2022. Quality Description Laser Data. Document Version: 1.6.

Le Coz, J., Renard, B., Bonnifait, L., Branger, F., Le Boursicaud, R., 2014. Combining hydraulic knowledge and uncertain gaugings in the estimation of hydrometric rating curves: a Bayesian approach. J. Hydrol. 509, 573–587.

Lee, M., Yoo, Y., Joo, H., Kim, K.T., Kim, H.S., Kim, S., 2021. Construction of rating curve at high water level considering rainfall effect in a tidal river. J. Hydrol.: Reg. Stud. 37, 100907.

Lehmkuhl, F., Schüttrumpf, H., Schwarzbauer, J., Brüll, C., Dietze, M., Letmathe, P., Völker, C., Hollert, H., 2022. Assessment of the 2021 summer flood in Central Europe. Environ. Sci. Eur. 34 (1), 107.

Lindström, G., Pers, C., Rosberg, J., Strömqvist, J., Arheimer, B., 2010. Development and testing of the HYPE (Hydrological Predictions for the Environment) water quality model for different spatial scales. Hydrol. Res. 41 (3-4), 295–319.

Liu, J., Feng, S., Gu, X., Zhang, Y., Beck, H.E., Zhang, J., Yan, S., 2022. Global changes in floods and their drivers. J. Hydrol. 614, 128553.

Lyddon, C., Robins, P., Lewis, M., Barkwith, A., Vasilopoulos, G., Haigh, I., Coulthard, T., 2023. Historic spatial patterns of storm-driven compound events in UK estuaries. Estuaries Coasts 46 (1), 30–56.

Martin-Gousset, H., Persson, K.M., Roy, D., 2009. Impact of effluents from lyby wastewater treatment plant on the nitrogen content of lake ringsjön and rönne Å river, sweden. VATTEN 65, 255–265.

Moftakhari, H.R., Salvadori, G., AghaKouchak, A., Sanders, B.F., Matthew, R.A., 2017. Compounding effects of sea level rise and fluvial flooding. Proc. Natl. Acad. Sci. 114 (37), 9785–9790.

MSB 2015. Översvämningskartering Utmed Höje Å. Rapport nr: 47, Myndigheten för samhällsskydd och beredskap, Sweden (in Swedish).

MTE 2020. Sjömätningsrappport, Ängelholms Kommun. Skälderviken och Rönne å. Rapport Rönne å, Ängelholms Kommun, Projektnummer 181019, MarCon Teknik AB, Malmö, Sweden (in Swedish).

Olbert, A.I., Moradian, S., Nash, S., Comer, J., Kazmierczak, B., Falconer, R.A., Hartnett, M., 2023. Combined statistical and hydrodynamic modelling of compound flooding in coastal areas-Methodology and application. J. Hydrol. 620, 129383.

Påsse, T. and J. Daniels 2015. Past shore-level and sea-level displacements, Sveriges geologiska undersökning (SGU), Rapporter och meddelanden 137.
Pender, G., Néelz, S., 2007. Use of computer models of flood inundation to facilitate communication in flood risk management. Environ. Hazards 7 (2), 106–114.
Persson, G., J. Andréasson, D. Eklund, K. Hallberg, S. Nerheim, E. Sjökvist, L. Wern and S. Åström 2011a. Klimatanalys för Västra Götalands län. SMHI Report, Rapport 45 (in Swedish).
Persson, G., E. Sjökvist, S. Åström, D. Eklund, J. Andréasson, A. Johnell, M. Asp, J. Olsson and S. Nerheim 2011b. Klimatanalys för Skåne län. SMHI rapport (2011-52): 88 (in Swedish).
Pinos, J., Timbe, L., 2019. Performance assessment of two-dimensional hydraulic models for generation of flood inundation maps in mountain river basins. Water Sci. Eng. 12 (1), 11–18.
R Core Team, 2013. R: A Language and Environment for Statistical Computing. R Foundation for Statistical Computing, Vienna, Austria. ⟨https://www.R-project.org/⟩.
Rantz, S.E., 1982. Measurement and Computation of Streamflow: Volume 1. Measurement of Stage and Discharge. Geological Survey Water-Supply Paper 2175. US Geological Survey, Washington DC.
Santos, V.M., Wahl, T., Jane, R., Misra, S.K., White, K.D., 2021. Assessing compound flooding potential with multivariate statistical models in a complex estuarine system under data constraints. J. Flood Risk Manag. 14 (4), e12749.
Sarchani, S., Tsanis, I., 2024. Climate change impact on flood inundation along the downstream reach of the Humber River basin. J. Hydrol.: Reg. Stud. 53, 101829.
Schanze, J., 2006. Flood risk management – A basic framework. In: Flood Risk Management: Hazards, Vulnerability, and Mitigation Measures. NATO Earth and Environmental Sciences, 67. Springer, Dordrecht, The Netherlands.
Sechu, G. 2015. Sediment transport in Säveån and its implications for erosion and bank stability. Master Thesis TVVR 15/5013, Division of Water Resources Engineering, Department of Building and Environmental Technology, Lund University, Lund, Sweden.
Shekhar, S., S. Bhagat, K. Sivakumar and B. Koteshwar Kolluri 2018. Dominance-Analysis: A Python Library for Accurate and Intuitive Relative Importance of Predictors. ⟨https://github.com/dominance-analysis/dominance-analysis⟩.
SMHI 2015. Accessed May 10, 2022. ⟨https://www.smhi.se/kunskapsbanken/meteorologi/stormar-i-sverige/enskilda-stormar-och-ovader/freja-gorm-och-helga-nov-dec-2015-1.104502⟩.
SMHI 2020a. Vattenwebb. Accessed November 10, 2020. ⟨https://vattenweb.se⟩.
SMHI 2020b. Data. Accessed November 15, 2020. ⟨https://www.smhi.se/data⟩.
SMHI 2022. Climate indicator – Sea level. Accessed August 15, 2024. ⟨https://www.smhi.se/en/climate/climate-indicators/climate-indicators-sea-level⟩.
SMHI 2024. Storms in Sweden. Accessed July 30, 2024. ⟨https://www.smhi.se/kunskapsbanken/meteorologi/stormar-i-sverige⟩.
Sopelana, J., Cea, L., Ruano, S., 2018. A continuous simulation approach for the estimation of extreme flood inundation in coastal river reaches affected by meso-and macrotides. Nat. Hazards 93, 1337–1358.
Stoleriu, C.C., Urzica, A., Mihu-Pintilie, A., 2020. Improving flood risk map accuracy using high-density LiDAR data and the HEC-RAS river analysis system: a case study from north-eastern Romania. J. flood risk Manag. 13, e12572.
Sugg, M.M., Runkle, J.D., Ryan, S.C., Wertis, L., 2023. A difference-in difference analysis of the South Carolina 2015 extreme floods and the association with maternal health. Int. J. Disaster Risk Reduct. 97, 104037.
Sun, Y., Zhang, Q., Singh, V.P., 2024. Flooding in the Yellow River Basin, China: spatiotemporal patterns, drivers and future tendency. J. Hydrol.: Reg. Stud. 52, 101706.
Svensson, C., Jones, D.A., 2002. Dependence between extreme sea surge, river flow and precipitation in eastern Britain. Int. J. Climatol.: A J. R. Meteorol. Soc. 22 (10), 1149–1168.
Svensson, C., Jones, D.A., 2004. Dependence between sea surge, river flow and precipitation in south and west Britain. Hydrol. Earth Syst. Sci. 8 (5), 973–992.
Takayama, R., Nakamura, R., Esteban, M., Mäll, M., Ohizumi, K., 2023. Pseudo global warming experiment of flood inundation in the upper White Volta River, Ghana. J. Hydrol.: Reg. Stud. 45, 101297.
Tayefi, V., Lane, S., Hardy, R., Yu, D., 2007. A comparison of one-and two-dimensional approaches to modelling flood inundation over complex upland floodplains. Hydrol. Process.: Int. J. 21 (23), 3190–3202.
Ward, P.J., Couasnon, A., Eilander, D., Haigh, I.D., Hendry, A., Muis, S., Veldkamp, T.I., Winsemius, H.C., Wahl, T., 2018. Dependence between high sea-level and high river discharge increases flood hazard in global deltas and estuaries. Environ. Res. Lett. 13 (8), 084012.
Ward, P.J., De Moel, H., Aerts, J., 2011. How are flood risk estimates affected by the choice of return-periods? Nat. Hazards Earth Syst. Sci. 11 (12), 3181–3195.
Yi, Y., Liu, S., Zhang, X., Yang, Y., Zhu, Y., Cui, F., Wu, K., Xie, F., 2023. Spring floods and their major influential factors in the upper reaches of Jinsha River basin during 2001–2020. J. Hydrol.: Reg. Stud. 45, 101318.